NASA TECHNICAL NOTE

NASA TN D-3389

NASA TN D-3389

PHOTOMETRIC ANALYSIS OF SPECTROGRAMS OF TWO TRAILBLAZER I PAYLOAD REENTRY EVENTS

by Gale A. Harvey

Langley Research Center
Langley Station, Hampton, Va.

NATIONAL AERONAUTICS AND SPACE ADMINISTRATION • WASHINGTON, D. C. • APRIL 1966

NASA TN D-3389

PHOTOMETRIC ANALYSIS OF SPECTROGRAMS OF TWO TRAILBLAZER I PAYLOAD REENTRY EVENTS

By Gale A. Harvey

Langley Research Center
Langley Station, Hampton, Va.

NATIONAL AERONAUTICS AND SPACE ADMINISTRATION

For sale by the Clearinghouse for Federal Scientific and Technical Information
Springfield, Virginia 22151 – Price $0.35

PHOTOMETRIC ANALYSIS OF SPECTROGRAMS OF TWO TRAILBLAZER I PAYLOAD REENTRY EVENTS

By Gale A. Harvey
Langley Research Center

SUMMARY

Slitless spectroscopy as a data system has yielded quantitative information on the reentry processes. Spectral photometry of the reentry events of the payloads of Trailblazer Ii and Ik is presented. The radiation consisted of sodium, aluminum oxide, and continuum radiation in the red region of the spectrum. The altitude variation and the effect of sodium chloride seeding of the Trailblazer Ik payload are discussed. Aluminum oxide and nitrogen comparison spectra are presented.

INTRODUCTION

The Trailblazer I program was a cooperative effort between the National Aeronautics and Space Administration and the Massachusetts Institute of Technology Lincoln Laboratory. This program consisted mainly of obtaining radar cross-sectional data and optical data, both nondispersed and spectral, of the reentry process of Trailblazer I payload. The reentries were observed from ground-based radar and optical stations. The program used a unique six-stage solid-fuel rocket vehicle to reenter small payload weights in the ICBM velocity range. A description of the vehicle used in this investigation together with some flight tests results is given in references 1 and 2.

Low levels of radiation at the source, due primarily to the small size, low velocity (less than 6 kilometers per second), and low reentry elevation angles from the optical sites, and reentry-camera distances of 100 to 200 kilometers have characterized the reentries. However, evolution of slitless spectrographs and field application technique have resulted in usable spectral data from two payload reentry events.

The reduction and interpretation of spectrograms of the Trailblazer Ii and Ik payload reentries are the subject of this paper.

VEHICLE, PAYLOAD, AND SLITLESS SPECTROGRAPHS

The Trailblazer I vehicle is a six-stage solid-propellant vehicle. The first three stages, a standard Honest John M6 booster, a standard Nike M5 booster, and TX77 rocket motor, are used in tandem to position a velocity package in space at an altitude of approximately 300 kilometers. The velocity package contains the remaining three stages: a T-40 rocket motor, a T-55 rocket motor, and a Cygnus 5 12.7-centimeter-diameter spherical rocket motor which are used to give the payload the reentry velocity. Figure 1(a) is a sketch of a typical Trailblazer I launch vehicle, and figure 1(b) is a sketch of a typical velocity package.

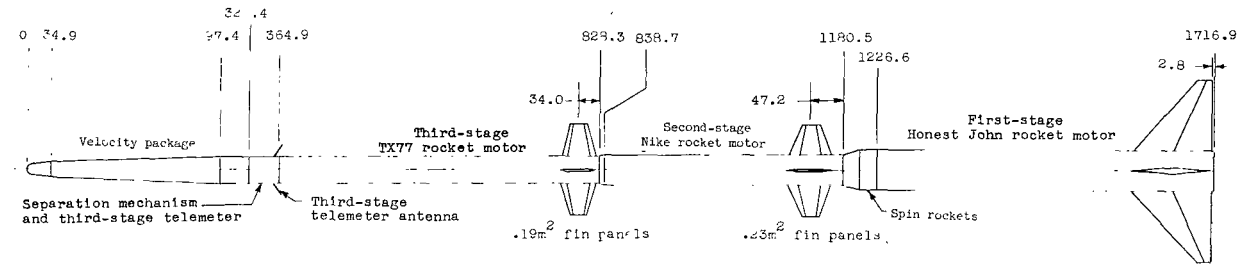

(a) Launch vehicle.

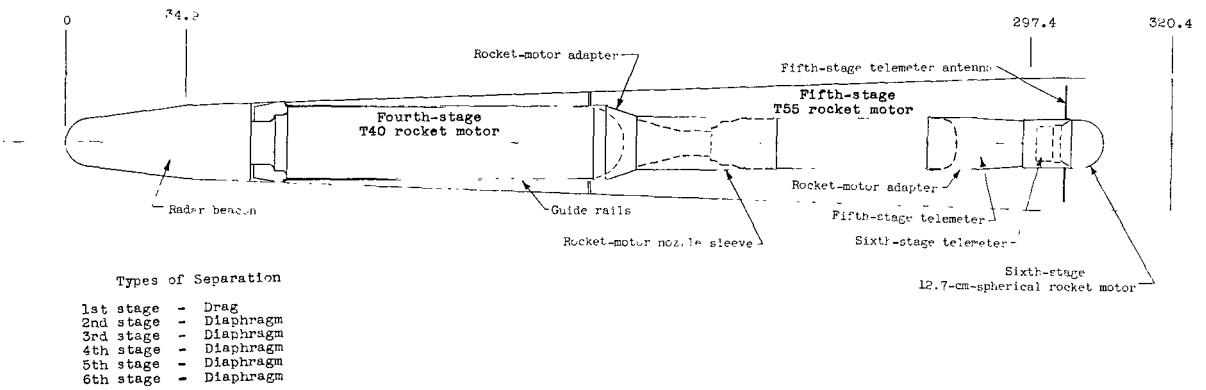

(b) Velocity package.

Figure 1.- Sketch of typical Trailblazer I launch vehicle and velocity package. All dimensions and station locations are in centimeters.

Sketches of the 12.7-centimeter-diameter spherical rocket-motor cases, which were the reentry payloads of Trailblazers Ii and Ik, are presented in figure 2. The Trailblazer Ii reentry payload (fig. 2(a)) was an exhausted aluminum 12.7-centimeter-diameter spherical rocket motor with a cylindrical shell around the nozzle. The Trailblazer Ik payload (fig. 2(b)) was an exhausted 12.7-centimeter-diameter spherical rocket motor with a layer of plastic foam impregnated with 15 grams of NaCl encased in

a thin aluminum 20.32-centimeter-diameter spherical shell. Given in table I is pertinent information on these reentry payloads. Velocity and altitude data determined from optical ballistic data are presented in table II.

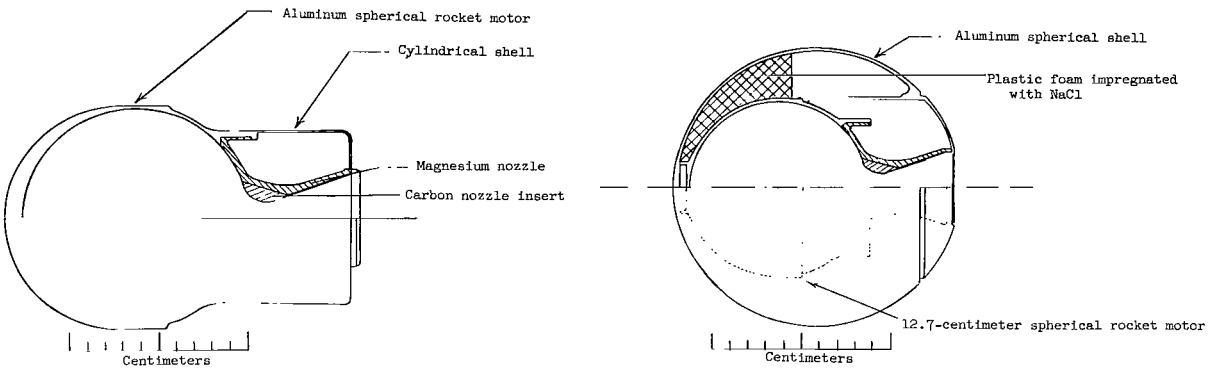

(a) Trailblazer Ii payload.

(b) Trailblazer Ik payload.

Figure 2.- Sketches of Trailblazer Ii and Ik reentry payloads.

The ground-based spectral-recording instruments were optically fast, short-focal-length cameras with objective dispersing elements. A Super Meteor Schmidt camera with a plastic objective prism and aerial K-24 cameras with objective diffraction gratings were used to obtain low-dispersion spectrograms of the reentry events. A description of the optical system of the 203-millimeter focal length, 54° circular field of view, f/.8, Super Schmidt camera is presented in reference 3. This camera with a polystyrene plastic prism provides spectrograms of inverse dispersion of about 700Å/mm. The f/2.5 K-24 aerial cameras have a square field of view of 40° and a focal length of 178 mm. Blazed first-order-transmission diffraction gratings of 75 lines/mm are mounted in front of the lenses of the K-24 aerial cameras. The inverse dispersion of a K-24 spectrograph with a 75 line/mm grating is approximately 730Å/mm. Kodak Royal X Panchromatic Film, which contains an ultra-high-speed ASA 1250 panchromatic emulsion, is used as the recording medium in spectral cameras. Figure 3 is a photograph of a K-24 aerial camera equipped with a transmission diffraction grating. The useful spectral range of these instruments is from 3900Å to 6500Å.

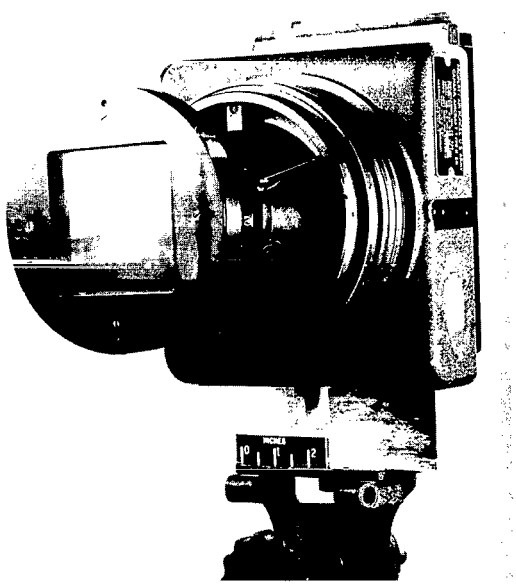

L-62-5897

Figure 3.- K-24 aerial camera with objective diffraction grating.

DATA REDUCTION PROCEDURE

The reduction of the reentry spectrograms consists of two parts: determination of the wavelength of the radiation and determination of the intensity of the radiation as a function of wavelength, that is, the spectral irradiance. The method used for the wavelength reduction for the grating spectrograms was to obtain an approximate dispersion scale from the grating equation:

$$d(\sin \theta + \sin i) = n\lambda$$

where

d	spacing between grooves in grating
θ	angle between optical axis and dispersed radiation
i	angle between optical axis and zero order
n	order number
λ	wavelength of radiation

This dispersion scale is then checked with a mercury-cadmium (Hg - Cd) spectrum taken with the reentry camera and adjusted to agree with known features in a particular spectrum, for example, the sodium D lines. Each spectrogram must have a different scale constructed for each part of the spectrum reduced because the sin i dependence will cause the dispersion to vary by as much as 10 percent across the film plane. A densitometer tracing of the spectrum provides an expanded dispersion scale and enhances contrast of the image. Reference 4 was used to identify elements of line emission and reference 5 was used for identification of the molecular species of band emission.

The spectral photometry of the Trailblazer Ii reentry spectrogram was performed by Dr. Allan F. Cook of the Harvard College Observatory. The pertinent information on this photometry is presented in the appendix.

The spectral photometry of the Trailblazer Ik reentry spectrogram was performed by the method of Dr. Allan F. Cook which is described in references 6 and 7, where absolute spectral photometry has been performed on natural meteor spectrograms. In this method an intensity step wedge is impressed upon film by a sensitometer and this film is processed at the same time as the data film and provides the relative response of the film to radiation. The spectrograms are then calibrated against a stellar standard of spectral irradiance and corrections are made for differences in optical path and reciprocity failure. However, a suitable spectral sensitometer for the K-24 spectrographs did not exist at the

time of the Trailblazer I reentries, and hence no intensity step-wedge film with the same processing as the data film processing exists. Hence, an ex-post-facto calibration had to be used in the photometry of the Trailblazer Ik spectrogram. Irradiance from the star α Andromedae was recorded on the Ik spectrogram. The standard relationship, atmospheric extinction equals K secant z, where z is the zenith angle and K is a constant was applied to account for the difference in zenith angle, 3^{o}, between α Andromedae and the reentry. The energy distribution from α Andromedae outside the earth's atmosphere was obtained from reference 8, and the stellar magnitude was obtained from reference 9. A reciprocity failure correction of 3.5, obtained by the method of reference 6, was applied.

RESULTS AND DISCUSSION

Ii Spectrum

The spectrum of the reentry event of the payload of Trailblazer Ii was recorded on a K-24 aerial camera equipped with a 75 line/mm diffraction grating and the Super Schmidt camera with a plastic prism. The K-24 camera was in motion during the reentry event in order that the trailing velocity of the reentry across the film plane might be low. In fact, the angular velocity of the camera was greater than the angular velocity of the reentry event across the sky, and the reentry event therefore appears inverted on the negative. The spectrogram from the Ii payload is presented in figure 4(a), and a nondispersed photograph of the same reentry event is presented in figure 4(b). The three flares in figure 4(a) are assumed to be the corresponding flares noted in figure 4(b). Figures 5(a), (b), and (c) present densitometer tracings of the three flares, and figure 5(d) is a panchromatic light curve of the reentry event. The positions and profiles of the aluminum oxide (AlO) band systems were obtained by joining the band head intensities presented in reference 5. In general, the distribution of energy within the bands depends upon the conditions of excitation and probably will be shifted to the right of the indicated profiles in figures 5(a), (b), and (c) because the AlO bands are degraded to the red. The light curve (fig. 5(d)) represents the nondispersed light, not corrected for reciprocity failure, response of a ballistic camera and panchromatic film to the reentry event. The light curve is plotted in absolute meteor magnitudes and indicates the intensity of the reentry event as a function of time. Spectrophotometry on the Ii reentry-event spectrogram from the Super Schmidt camera has been performed by Dr. Allan F. Cook at the Harvard College Observatory and is presented in figure 6. Pertinent information concerning the photometry is contained in the appendix.

The altitude agreement between figures 5(a) and 6(a), 5(b) and 6(b), and 5(c) and 6(c) is not exact and is probably a result of the difference in ballistic workups done by NASA and the Harvard College Observatory. The two sets of figures are quite consistent with each other in the range from 4800Å to 5500Å, but the K-24 spectrogram, the sensitivity

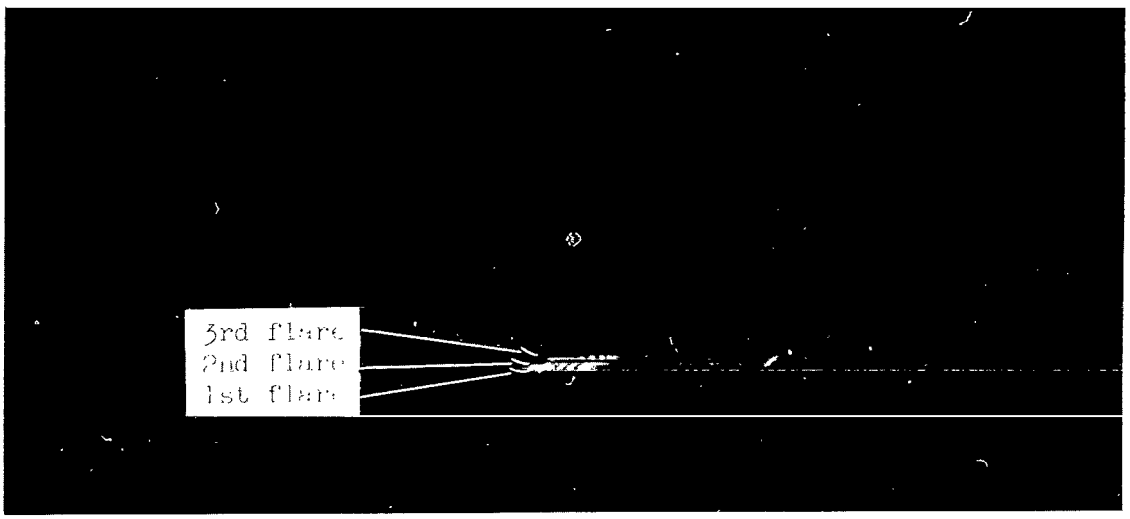

(a) Ii spectrogram.

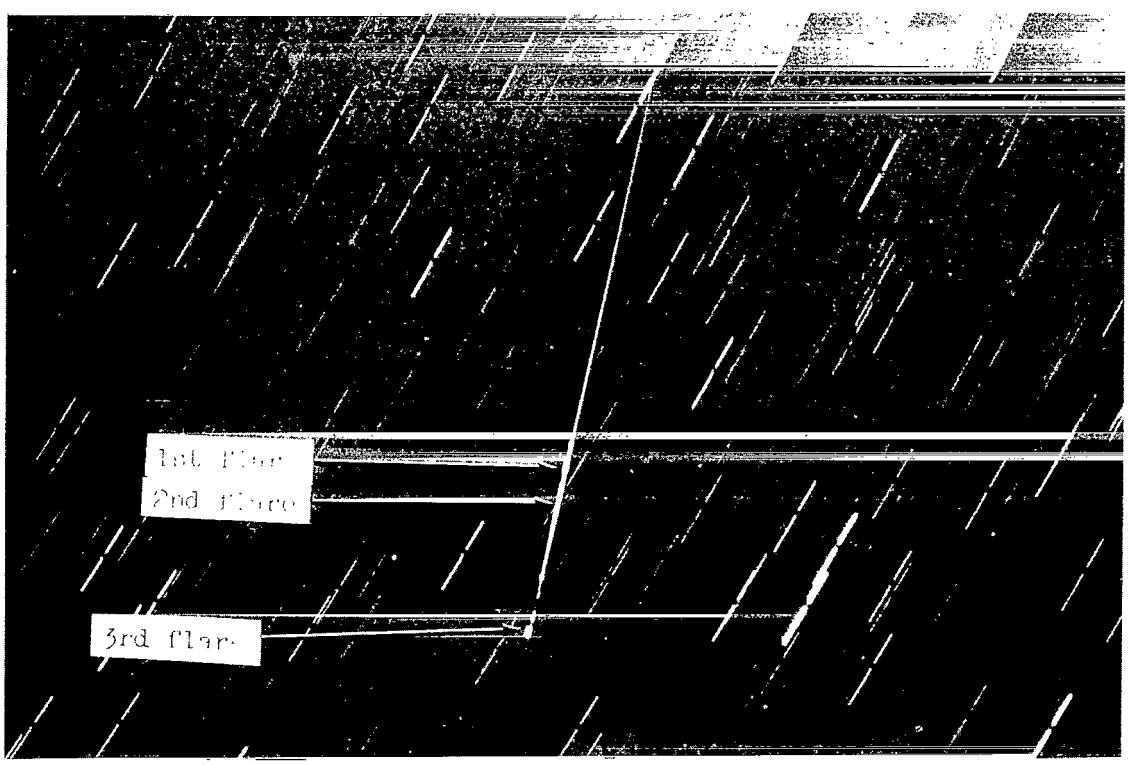

(b) Ii reentry photograph. L-65-7969

Figure 4.- Enlargements of K-24 spectrogram and ballistic camera photographs of Trailblazer Ii reentry event.

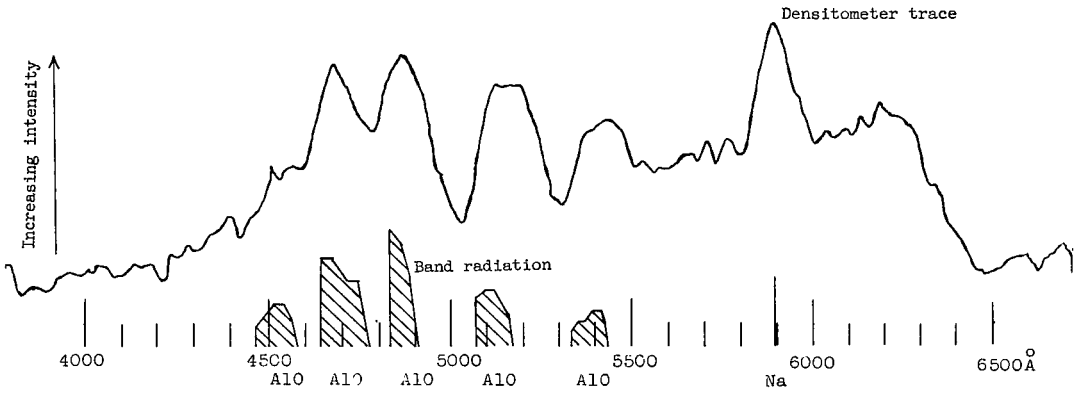

(a) 43.8 km.

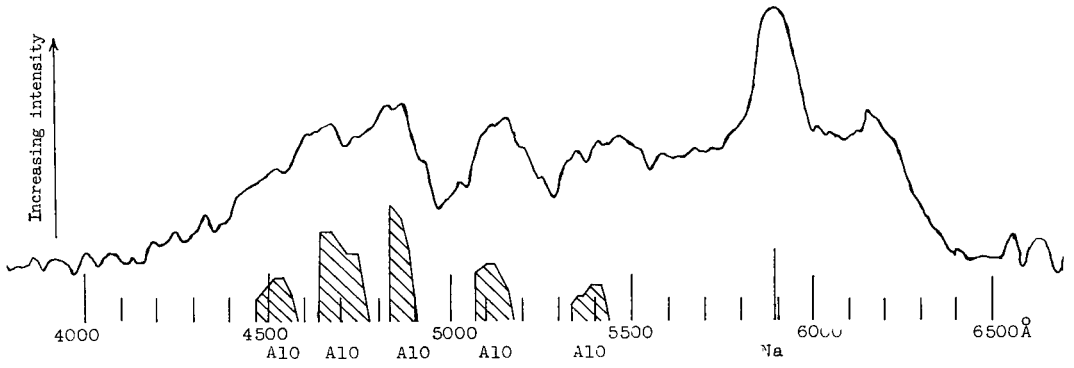

(b) 43.5 km.

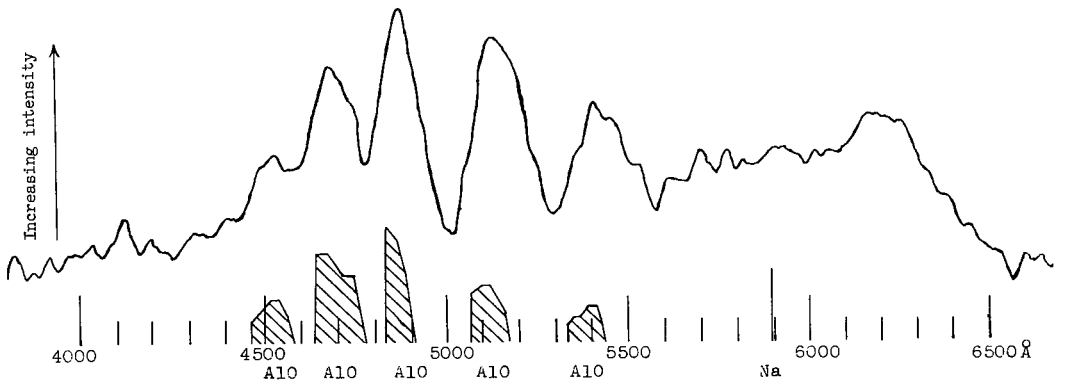

(c) 41.8 km.

Figure 5.- Densitometer tracings at various altitudes for K-24 spectrogram and panchromatic light curve of reentry for Trailblazer II. Positions of AlO and Na are noted.

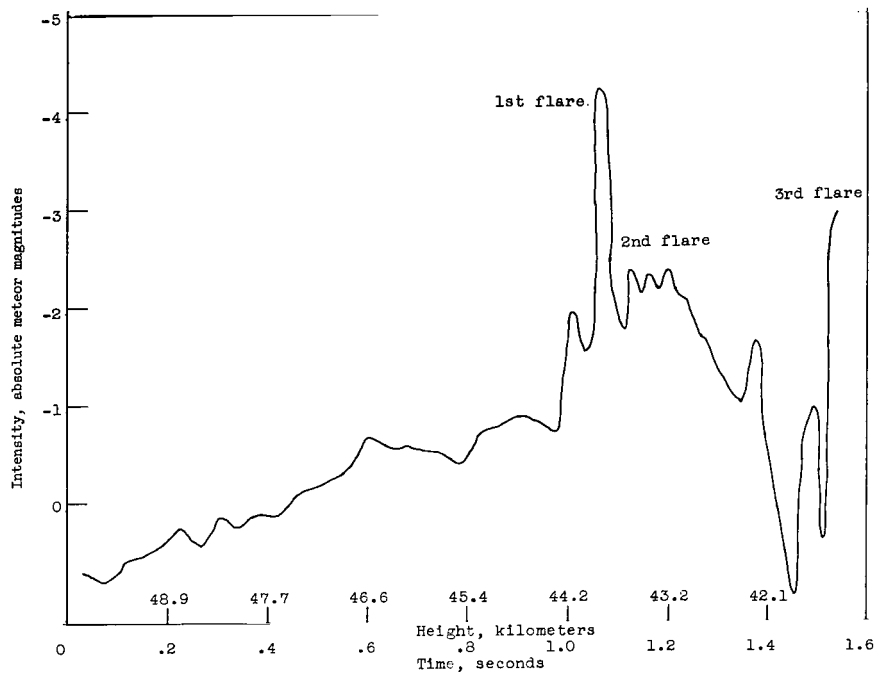

(d) Panchromatic light curve of Trailblazer Ii reentry.

Figure 5.- Concluded.

of which is roughly constant in the region from 4500Å to 6300Å, indicates more flux from the reentry event in the region from 5500Å to 6500Å. This difference is very noticeable for the sodium doublet which appears strong in figures 5(a) and (b), but is virtually absent in figures 6(a) and (b). The optimum focus as a function of wavelength was probably quite different for the two cameras, the Super Schmidt cameras are usually focused for blue light and the K-24 cameras are focused for yellow light, with a resulting loss in sensitivity for the out-of-focus region of the spectrum. This focus sensitivity loss and the lower look angles of the reentry from the Super Schmidt site, resulting in atmospheric H_2O absorption, are probably responsible for the loss of sensitivity in the Super Schmidt spectrogram in the region from 5500Å to 6500Å.

The first two flares (fig. 4) have heavy contributions from the sodium doublet (5890Å, 5896Å) and have aluminum oxide band radiation in the region from 4500Å to 5500Å and unresolved radiation, that is, an apparent continuum, in the red. The final flare consists predominately of the aluminum oxide radiation with some continuum and essentially no sodium radiation. The resolution of this spectrogram is about 20Å. It is noted that the so-called continuum does not have any identifiable structure and that no atomic aluminum lines are present.

Reference 10, a theoretical work, was used to determine what air emission species could be responsible for the unresolved radiation. The only two mechanisms treated in reference 10 which could approximate the distribution recorded on the spectrogram for temperatures between 3000° K and 9000° K and density ratios (emission gas density

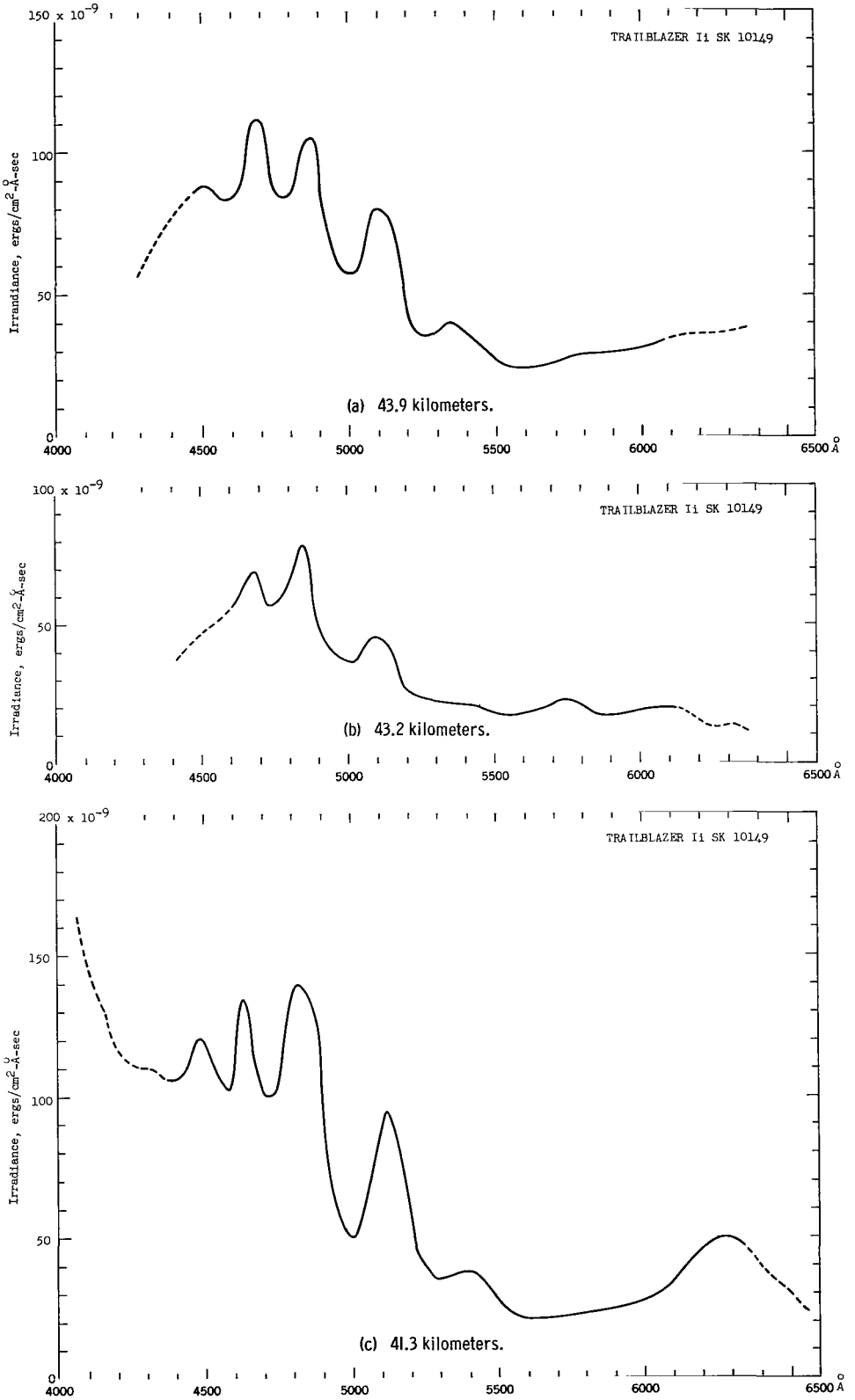

Figure 6.- Spectral irradiance from Trailblazer Ii 100 kilometers from the source at various altitudes obtained from Super Schmidt spectrograph.

divided by density of air at sea level) of 10^{-3} and 10^{+2} were the first positive nitrogen band system and oxygen free-free emission. Figure 7 is an enlargement of and a densitometer tracing of a spectrogram obtained by photographing light from a nitrogen filled Geissler tube with the same slitless spectrograph that recorded the spectra of figure 5. Identifiable structure, as shown in figure 7, would have been observed if the continuum radiation were solely from the first positive band system of nitrogen. Therefore the

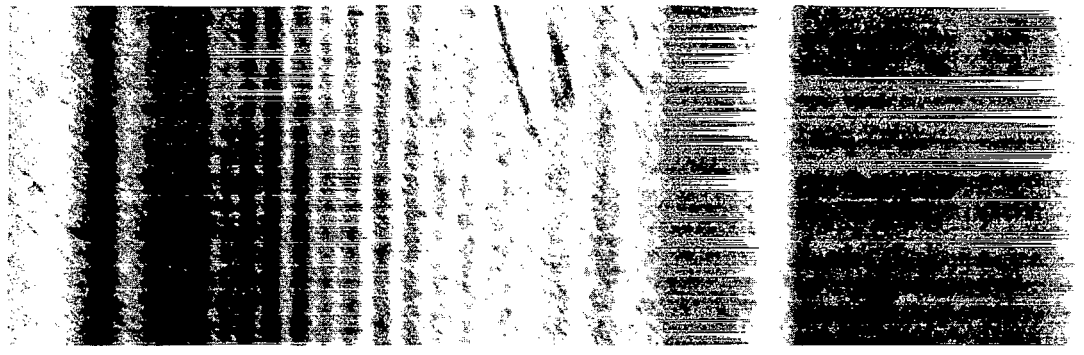

(a) Enlargment of N_2 spectrogram. X 42. L-65-7970

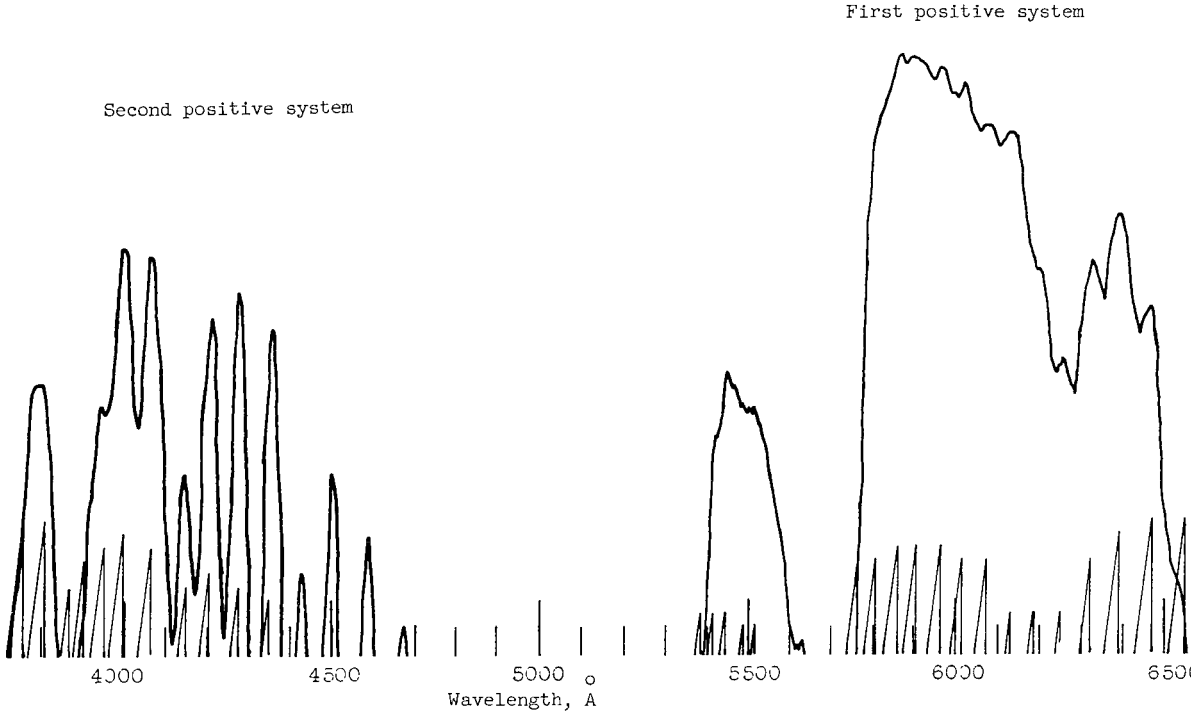

(b) Densitometer tracing of N_2 spectrogram.

Figure 7.- Enlargement and densitometer tracing of Geissler tube excited spectrogram. (Positions of strongest N_2 bands noted.)

continuum cannot be attributed to nitrogen (N_2). Oxygen free-free emission is not considered possible because (a) the conditions necessary for this emission would support emission, which is not observed, from several other species of gas and (b) the conditions of high temperature (6000° K) and high-density ratio (density ratio > 0.1) are not met by this reentry.

Two other possible explanations of the unresolved radiation are blackbody radiation from liquid drops of material in the wake and radiation from the reaction

$$NO + O \rightarrow NO_2 + h\nu$$

where h is Planck's constant $\left(6.6254 \times 10^{-27} \text{ erg-sec}\right)$ and ν is the frequency.

Blackbody radiation calculations do not indicate that blackbody radiation is the probable source of the continuum. A rough value for the energy in the continuum can be obtained by correlating figures 5(a), (b), and (c) with figures 6(a), (b), and (c) and using the fact that the K-24 spectrogram sensitivity at 6000Å is probably within a factor of 2 of the sensitivity at 5000Å. By using the values of 50×10^{-9} erg/cm^2-Å-sec, an average value of irradiance at 6000Å taken from figures 6(a), (b), and (c), for irradiance at 100 kilometers at 6000Å, a temperature of 2400° K (the boiling temperature of aluminum) for the drops, and a blackbody radiant emittance at the source of 2×10^4 ergs/cm^2-Å-sec at 6000Å (Emissivity = 1), it is determined that a total normal emissive area of 100 cm^2 is required to produce the irradiance recorded by the K-24 spectrogram. It is believed that an emissive area this large, which definitely represents a lower limit, is unrealistic for the payload and reentry condition of this experiment.

Wurster has published, in reference 11, an intensity distribution for the $NO + O \rightarrow NO_2 + h\nu$ reaction. The intensity increases from 5800Å to a peak at 6400Å for air at 3700° K. Since the observed energy distribution is similar to that of reference 11 in the region from 5800Å to 6400Å and the gas conditions (Temperature = 3700° K and density ratio < 0.1) are compatible with the temperatures expected for the near wake of this reentry, this low-temperature air radiation is probably the observed continuum radiation.

Ik Spectrum

Spectral photometry as discussed in the section entitled "Data Reduction Procedure" has been performed on a spectrogram of Trailblazer Ik. The K-24 spectrogram of the Ik payload reentry is presented in figure 8(a), and a nondispersed photograph of the reentry event is presented in 8(b). The results of the photometry and the light curve of the reentry are presented in figure 9. The contour lines in figures 9(a), (b), and (c) indicate the transmission and response of the atmosphere, optics, and film as a function of wavelength to different intensities of irradiance. The photograph in figure 8(b) and resulting light

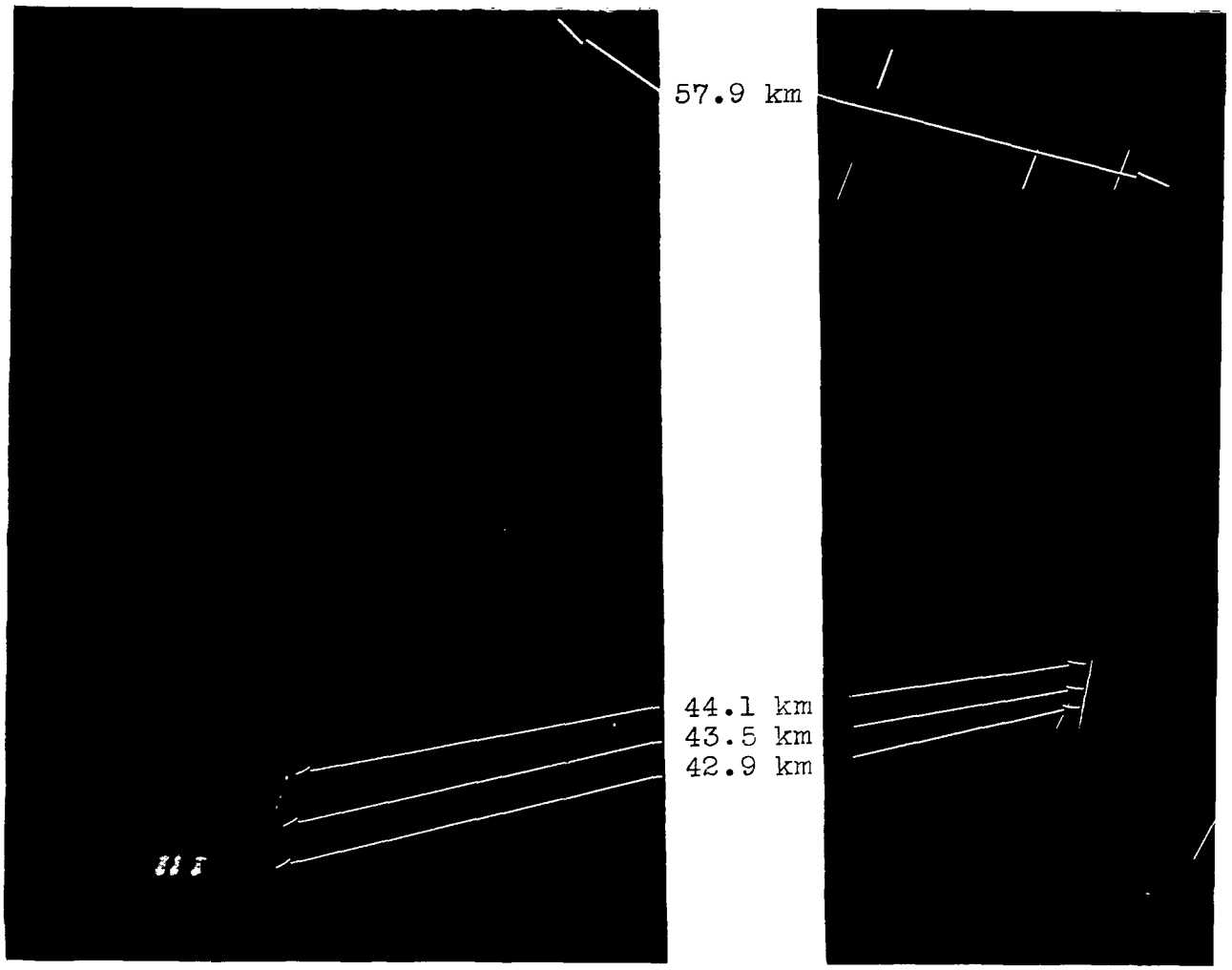

(a) Spectrogram.

(b) Nondispersed.

Figure 8.- Enlargements of K-24 spectrogram and ballistic camera photographs of Trailblazer Ik reentry event. L-65-7971

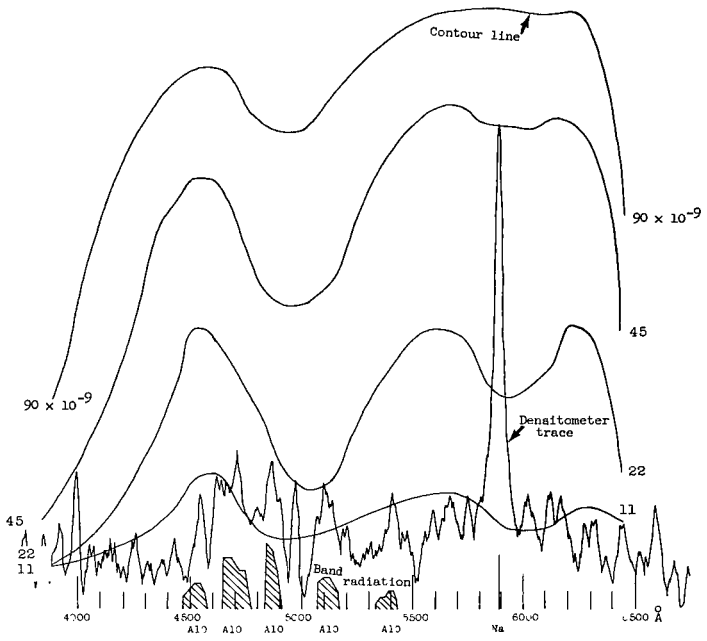

(a) 44.1 km.

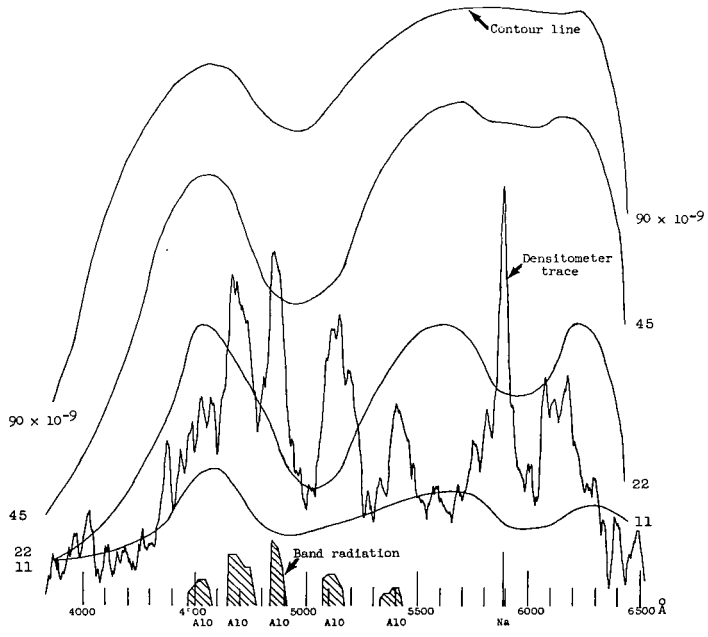

(b) 43.5 km.

Figure 9.- Spectral irradiance at various altitudes and panchromatic light curve of reentry for Trailblazer Ik. (Positions of AlO and Na emission noted.) Contour lines represent constant irradiance in ergs/cm^2-Å-sec at a distance of 100 km from the source.

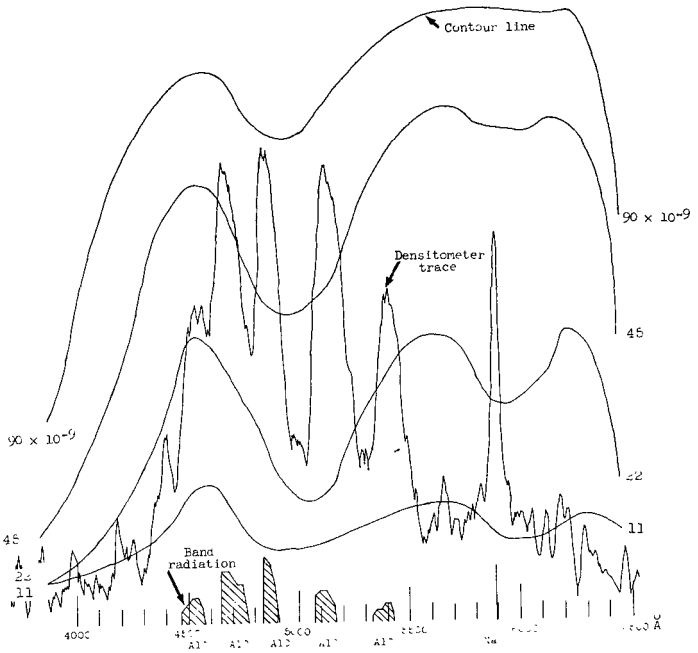

(c) 42.9 km.

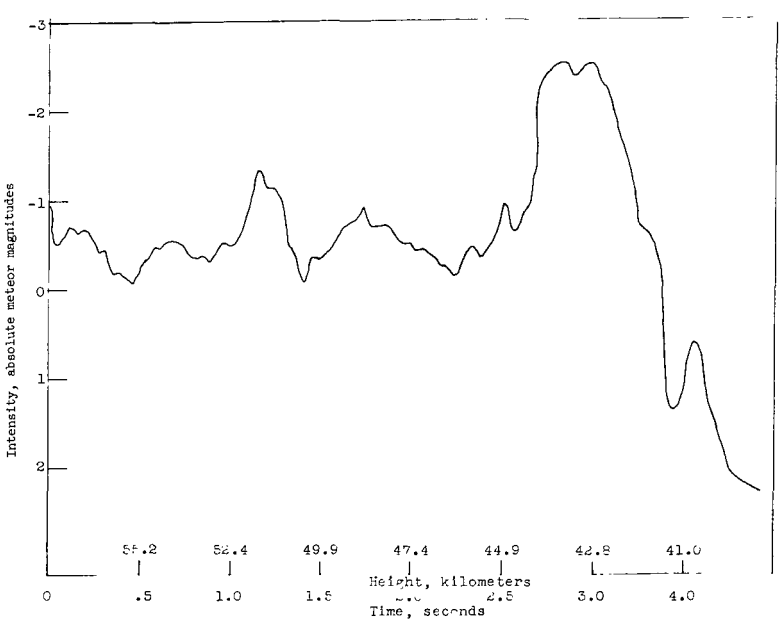

(d) Panchromatic light curve of Trailblazer Ik reentry.

Figure 9.- Concluded.

curve in figure 9(d) show faint emission from an altitude of 57.9 km to 44.1 km. At 44.1 km, the emission becomes much brighter and reaches a maximum at 43.5 km. The spectra of the event (fig. 8(a)) show that the faint radiation was predominantly due to sodium. At 44.1 km the sodium doublet becomes much brighter and aluminum oxide band emission begins. As the payload proceeds lower into the atmosphere, the band emission increases to a maximum at 42.9 km and then decreases. The sodium emission decreases from the maximum at 44.1 km. Continuum radiation in the range from 5600Å to 6500Å appears in the altitude interval from 43.5 km to 42.9 km.

The emission characteristics may be used to interpret the physical change of the Ik reentering body. The initial emission is from the 2.1-eV electron transition 3^2P to 3^2S of excited sodium atoms from the same sodium source as that for Ii payload, that is, from contamination, either from the atmosphere or from the payload. (The velocity package was exposed to the sea air on the launcher which is approximately 30.5 meters from the beach.) At 44.1 km, the Al case was burned through by aerodynamic heating and NaCl impregnated foam was exposed to the airstream. Consequently a large amount of sodium emission is recorded at this point. At about the same time, the rate of ablation of aluminum has increased sufficiently to allow AlO band radiation to be recorded. The ablation rate rapidly reaches a maximum with the corresponding radiation in the aluminum oxide bands and then declines as the payload decelerates and disintegrates. The intensity plots in figures 9(a), (b), and (c), are presented for three altitudes. Again it is noted that the atomic aluminum lines are not positively recorded, although the densitometer trace in figure 9(a) indicates possible identification of atomic aluminum lines at 3944Å and 3962Å near the film threshold. The continuum radiation in the red is a much weaker contributor for Ik than for Ii. Two factors that might lead to this result are the slightly lower velocity of Ik and the larger nose radius which would indicate a cooler stagnation point and a cooler wake.

These spectra can be compared with the aluminum oxide spectra presented in figure 10. This spectrum was obtained by burning chips of the aluminum stock from which the Ik payload was machined in a low-current dc arc and photographing the slit through which light from this arc passed. This was the same optical arrangement which was used to obtain figure 7, but with the substitution of the arc source for the N_2 Geissler tube. The energy distribution between the AlO band systems of the reentry radiation is not unlike the distribution of the arc-excited AlO radiation. However, the atomic aluminum lines at 3944Å, 3962Å are quite strong in the arc source. Atomic sodium radiation is also present in the arc spectra. The sodium may result from contamination from handling, or may be present as an impurity in the sample (400 ppm), or both. In any event, the atomic sodium radiation in the first flares of the Ik reentry is too intense, relative to the AlO radiation, to have much contribution from the aluminum material of the payload.

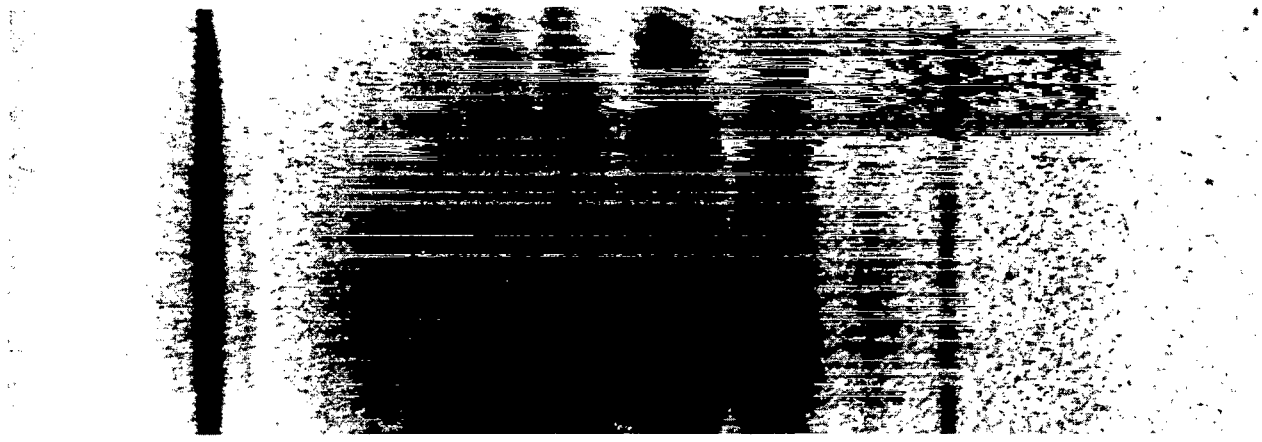

(a) Enlargement of AlO spectrogram. X 42. L-65-7972

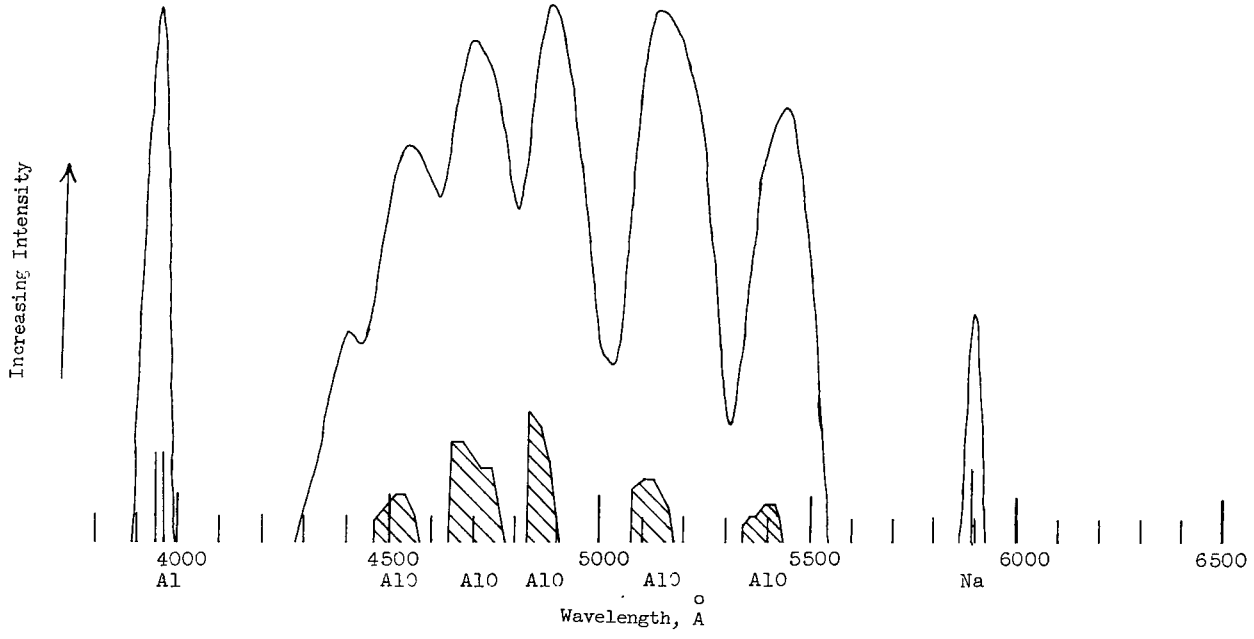

(b) Densitometer tracing of AlO spectrogram.

Figure 10.- Enlargement and densitometer tracing of dc arc excited aluminum oxide spectrogram. (Positions of Al, AlO, and Na emission noted.)

An indication of the efficiency with which the salt was excited can be obtained by integrating to find the total amount of energy in the Na doublet of the flares and dividing this value by the amount of energy from one electron transition. This number is 0.26×10^{21} ergs and compares with 1.5×10^{23} ergs for 15 grams of salt. An efficiency of 0.62 percent was thus obtained for the sodium excitation.

High accuracy in absolute spectral photometry, ±5 percent, can be obtained by sophisticated instrumentation and techniques used by leading professional astronomers. Slitless spectral photometry with moderate instrumentation and technique generally can be performed with an accuracy of about ±20 percent. The spectrograms discussed herein were obtained under conditions which greatly limited the accuracy of the photometry performed. Because one or two sources of error dominate the final accuracy of the photometry, a discussion of these predominant error sources is presented.

Possible nonuniform development of the Super Schmidt spectrograms and lack of a standardized star on the calibration spectrogram, as discussed in the appendix, are the two conditions which limit the accuracy of the data presented in figures 6(a), (b), and (c). Although Dr. Allan F. Cook does not state what the percent error is in the Super Schmidt photometry it is unlikely that the two preceding conditions would produce an error of more than -50 percent or +100 percent. The nonsymmetrical error is accounted for by the generally logarithmic response of film to radiant energy.

The use of an ex-post-facto calibration on the K-24 spectrogram is the condition which limits the accuracy on the Trailblazer Ik photometry. This condition would introduce no error if the densities of the standardized star first-order image and the reentry first-order image were the same. The densities of both the star and the reentry first-order images ran from about 0.1 to 0.5 above gross fog. The calibration film with the density step wedge was the same type of film as that used for the Ik spectrogram and the developing procedure for the two films was the same. Considering the density range covered, it is improbable that differences in emulsion batches and film processing coupled with the usual errors of photometry could have produced errors larger than -50 percent and +100 percent. The spectral photometry presented in this paper represents relatively unrefined measurements of the spectral irradiance from two Trailblazer I reentry events.

CONCLUDING REMARKS

A reduction and limited interpretation of spectrograms of two Trailblazer I payload reentry events have been presented and represent initial quantitative spectral data from reentering bodies in the ICBM velocity range.

Slitless spectroscopy has been used to obtain data of the atmospheric reentry process. The spectrograms treated in this investigation revealed the following information:

(a) The radiation in the region from 3900Å to 6500Å from the Trailblazer Ii reentry was primarily from the sodium doublet, aluminum oxide bands, and continuum radiation from low-temperature air.

(b) The radiation in the region from 3900Å to 6500Å from the Trailblazer Ik reentry was primarily from the sodium doublet and aluminum oxide band radiation.

(c) Sodium chloride seeding proved to be a feasible method of determining time and altitude of burn through of a payload.

Langley Research Center,
National Aeronautics and Space Administration,
Langley Station, Hampton, Va., December 3, 1965.

APPENDIX

PHOTOMETRY OF SUPER SCHMIDT SPECTROGRAM OF TRAILBLAZER Ii REENTRY

Spectral photometry of the Super Schmidt prismatic spectrogram of the Trailblazer Ii payload reentry event has been performed at Harvard College Observatory under contract to M.I.T. Lincoln Laboratory. Richard E. McCrosky was the scientist-in-charge, and the photometry was performed by Allan F. Cook. The following information is from the Report for February, 1963 (AF19(604) 7400, Sub. 234) from Harvard College Observatory to M.I.T. Lincoln Laboratory.

No standard stars were available on the Trailblazer Ii Super Schmidt spectrogram, SK 10149 (see fig. 6), because the camera was driven during that exposure. Trailed stellar spectra were available on the calibration spectrogram (SK 10150) which was developed in the same tank at the same time. There is real suspicion that development was not uniform from top to bottom of the tank. However, no reliable correction could be made for this.

None of the stars appearing on spectrogram SK 10150 have been measured for the intensity distribution in the stars continuum. Stars were selected solely on the basis of whether or not they provided good spectra for tracing and were not known variable stars. Two such stars were traced, τ Ceti and α Phoenicis.

No sensitometric steps were imprinted on either spectrogram SK 10149 or 10150. These steps were imprinted weeks later on a film from the same molding batch which was developed with the same developing solutions. This circumstance may introduce large errors in the results via the mean H and D curve adopted. The variation of this curve with wavelength was not large enough to be a serious problem.

Dispersion curves for the spectra were established from spectrograms of mercury lamps, some with cadmium added. These lamps were mounted on a tower on Wallops Island, Virginia. Since bands of aluminum oxide could be identified in the spectrum of the reentry, the zero point of the dispersion curve could be fixed without ambiquity. For the two stars, the wavelength of the red cutoff of the intensity curve (steepest slope) was taken to be 6265Å. A check was then provided by the wavelengths of maximum intensity and of the green "dip" (really a flat portion of the curve) which fell at 5750Å and 4875Å.

Since intensity curves for τ Ceti and α Phoenicis are not available, the best that can be done is to use the magnitudes and colors given by MacRae (ref. 9, pp. 68-78) to establish the corresponding blackbody-radiation curves. This procedure works for α Lyrae within ± 25 percent. Corrections for extinction were applied to reduce the deduced sensitivity curves to the zenith distances of the reentry. The two stars gave consistent results

except at the blue end of the spectrum. The star τ Ceti was adopted as the standard because of the large extinction corrections required for α Phoenicis.

Figures 6(a), (b), and (c) exhibit the deduced absolute fluxes from the reentry which correspond to a range of 100 km.

REFERENCES

1. Gardner, William N.; Brown, Clarence A., Jr.; Henning, Allen B.; Hook, W. Ray; Lundstrom, Reginald R.; and Ramsey, Ira W., Jr.: Description of Vehicle System and Flight Tests of Nine Trailblazer I Reentry Physics Research Vehicles. NASA TN D-2189, 1964.

2. Brown, Clarence A., Jr.; and Keating, Jean C.: Flight Test Performance and Description of a Rocket Vehicle for Producing Low-Speed Artificial Meteors. NASA TN D-2270, 1964.

3. McKinley, D. W. R.: Meteor Science and Engineering. McGraw-Hill Book Co., Inc., 1961.

4. Harrison, George R., compiler: Massachusetts Institute of Technology Wavelength Tables. John Wiley & Sons, Inc., 1960.

5. Pearse, R. W. B.; and Gaydon, A. G.: The Identification of Molecular Spectra. Third ed., Chapman & Hall, Ltd. (London), 1963.

6. Cook, Allan F., and Millman, Peter M.: Photometric Analysis of a Spectrogram of a Perseid Meteor. Astrophys. J., vol. 121, no. 1, Jan., 1955, pp. 250-270.

7. Millman, Peter M.; and Cook, Allan F.: Photometric Analysis of a Spectrogram of a Very Slow Meteor. Astrophys. J., vol. 130, no. 2, Sept. 1959, pp. 648-662.

8. Kienle, Von H.; Strassl, H.; and Wempe, J.: Die relative Energieverteilung im kontinuierlichen Spektrum von 36 Fundamentalsternen. Z. Astrophys., Bd. 16, Nr. 4, 1938, pp. 201-275.

9. Northcott, Ruth J., ed.: The Observer's Handbook 1962. Roy. Astron. Soc. Can.

10. Breene, R. G., Jr.; and Nardone, Maria: Radiant Emission From High Temperature Equilibrium Air. R61SD020 (Contract No. AF04(647)269), Space Sci. Lab., Gen. Elec. Co., May 1961.

11. Wurster, Walter H.: Study of Infrared Emission From Hypersonic Air Flows. Rept. No. QM-1626-A-13 (Contract No. ARPA No. 253-62), Cornell Aeron. Lab., Inc., July 1963.

TABLE I.- PAYLOAD INFORMATION

Payload	Trailblazer Ii	Trailblazer Ik
Mass	0.6396 kg	1.179 kg
Material	Al, C, Mg	Al, C, Mg
Seeding	None	15 gm NaC1
Launch date	Sept. 26, 1961	July 27, 1962
Reentry velocity	5.9 km/sec	5.6 km/sec
Spectral coverage . . .	Super Schmidt 75 lines/mm K-24's	Super Schmidt Three 75 lines/mm K-24's

TABLE II.- ALTITUDE AND VELOCITY DATA FROM OPTICAL BALLISTIC DATA

Trailblazer Ii		Trailblazer Ik	
Altitude, kilometers	Velocity, km/sec	Altitude, kilometers	Velocity, km/sec
48.657	5.928	56.372	5.574
48.300	5.919	56.308	5.572
48.115	5.914	55.295	5.542
47.781	5.903	55.215	5.539
47.505	5.896	54.198	5.504
47.205	5.882	54.126	5.501
46.902	5.874	53.132	5.460
46.583	5.855	53.064	5.456
46.356	5.845	51.006	5.347
45.992	5.822	50.938	5.341
45.803	5.810	49.962	5.275
45.465	5.781	49.893	5.268
45.211	5.765	48.946	5.191
44.897	5.728	48.876	5.183
44.681	5.708	47.934	5.092
44.403	5.663	47.876	5.083
44.134	5.637	45.989	4.840
43.772	5.580	45.920	4.827
43.565	5.547	45.051	4.680
43.209	5.475	44.992	4.665
43.047	5.435	44.163	4.492
42.640	5.344	44.067	4.475
42.504	5.293	43.306	4.272
42.163	5.178	43.206	4.252
42.037	5.114	41.703	3.711
41.702	4.970	41.674	3.684
41.524	4.890	41.029	3.355
41.235	4.708	40.995	3.323
40.645	4.251		
40.337	3.964		

"The aeronautical and space activities of the United States shall be conducted so as to contribute . . . to the expansion of human knowledge of phenomena in the atmosphere and space. The Administration shall provide for the widest practicable and appropriate dissemination of information concerning its activities and the results thereof."

—NATIONAL AERONAUTICS AND SPACE ACT OF 1958

NASA SCIENTIFIC AND TECHNICAL PUBLICATIONS

TECHNICAL REPORTS: Scientific and technical information considered important, complete, and a lasting contribution to existing knowledge.

TECHNICAL NOTES: Information less broad in scope but nevertheless of importance as a contribution to existing knowledge.

TECHNICAL MEMORANDUMS: Information receiving limited distribution because of preliminary data, security classification, or other reasons.

CONTRACTOR REPORTS: Technical information generated in connection with a NASA contract or grant and released under NASA auspices.

TECHNICAL TRANSLATIONS: Information published in a foreign language considered to merit NASA distribution in English.

TECHNICAL REPRINTS: Information derived from NASA activities and initially published in the form of journal articles.

SPECIAL PUBLICATIONS: Information derived from or of value to NASA activities but not necessarily reporting the results of individual NASA-programmed scientific efforts. Publications include conference proceedings, monographs, data compilations, handbooks, sourcebooks, and special bibliographies.

Details on the availability of these publications may be obtained from:

SCIENTIFIC AND TECHNICAL INFORMATION DIVISION

NATIONAL AERONAUTICS AND SPACE ADMINISTRATION

Washington, D.C. 20546